Orbit-Determination Performance of Doppler Data for Interplanetary Cruise Trajectories Part I: Error Analysis Methodology

J. S. Ulvestad and S. W. Thurman
Navigation Systems Section

This article describes an error covariance analysis methodology used to investigate different weighting schemes for two-way (coherent) Doppler data in the presence of transmission-media and observing-platform calibration errors. The analysis focuses on orbit-determination performance in the interplanetary cruise phase of deep-space missions. Analytical models for the Doppler observable and for transmission-media and observing-platform calibration errors are presented, drawn primarily from previous work. Previously published analytical models have been improved upon by (1) considering the effects of errors in the calibration of radio signal propagation through the troposphere and ionosphere as well as station-location errors; (2) modelling the spacecraft state transition matrix using a more accurate piecewise-linear approximation to represent the evolution of the spacecraft trajectory; and (3) incorporating Doppler data weighting functions that are functions of elevation angle, which reduce the sensitivity of the estimated spacecraft trajectory to troposphere and ionosphere calibration errors. The analysis is motivated by the need to develop suitable weighting functions for two-way Doppler data acquired at 8.4 GHz (X-band) and 32 GHz (Ka-band). This weighting is likely to be different from that in the weighting functions currently in use; the current functions were constructed originally for use with 2.3-GHz (S-band) Doppler data, which are affected much more strongly by the ionosphere than are the higher frequency data.

I. Introduction

Interplanetary spacecraft navigation is accomplished using a number of different techniques. The classical means of navigation have included those based on measurements of Doppler shift and on ranging measurements. In recent years, differential very long baseline interferometry (VLBI) has been added to the arsenal of tools used for navigation [1]. For planetary approach and encounter, optical navigation using images of solar-system bodies against the background stars also is a very useful means of navigation [2]. Differenced (two-way minus three-way) Doppler

and range currently are being investigated for spacecraft tracking [3,4], as are other interferometric data types such as connected-element interferometry [5] and same-beam VLBI [6].

Despite the plethora of data types being developed, the workhorse navigation data type remains two-way (coherent) Doppler. These data are easy to acquire and can be obtained without interference with telemetry transmission from a spacecraft. However, fairly long tracking sessions ("passes") are necessary on each day of tracking. Doppler data are directly sensitive to motion along the line of sight; accumulation of Doppler data over a number of days provides increasing sensitivity to position and velocity in the plane of the sky (the plane perpendicular to the Earth–spacecraft line-of-sight). VLBI data yielding similar or improved *angular* accuracies often can be acquired in far less time at a greater operational cost and at the expense of interfering with telemetry transmission from the spacecraft. As instrumentation noise has been reduced and the calibration of various effects that cause systematic measurement errors has advanced, the orbit-determination performance obtained from Doppler data has improved substantially.

Obtaining the best accuracy from Doppler data often has required that an empirical trade-off be made between acquiring the most data possible in a given pass and down-weighting or deleting the data which can contain large errors due to imperfect calibration. In particular, it has been a common practice to deweight or discard data acquired at low elevation angles because of errors in the calibration of propagation effects in the Earth's ionosphere and troposphere. For Doppler data taken near 2.3 GHz (S-band), ionosphere calibration errors typically dominate the low-elevation data. Current missions often use the higher radio frequency of 8.4 GHz (X-band), and future missions may use transmission frequencies near 32 GHz (Ka-band) for improved telemetry performance. At these higher frequencies, the ionosphere calibration errors become less important (ionospheric propagation errors scale with the inverse square of the radio frequency), and troposphere calibration uncertainties dominate the errors in the low-elevation data. For Doppler data used in orbit determination, the weighting function currently implemented at JPL was established when radio metric data were obtained at 2.3 GHz and emphasized the minimization of errors caused by imperfect ionosphere calibration. Therefore this function is inappropriate for 8.4-GHz and 32-GHz data.

This article describes the development of a numerical error covariance analysis used to investigate the benefits of new elevation-dependent weighting schemes for Doppler data acquired at high radio frequencies. The analysis described below is applicable to interplanetary cruise trajectories, but does not include features to enable computation of gravitational effects encountered during planetary approach or encounter phases. A piecewise-linear approximation to the evolution of the spacecraft state vector enables the analysis to be applied to data arcs that are months in length; keeping quadratic terms could enable the study of even longer data arcs at the expense of much additional computation. The virtue of the piecewise-linear analysis is that it is relatively simple, enabling consideration of a large number of different cases in a short period of time.

Previous analytical and numerical studies of Doppler-based orbit-determination performance can be found in a number of different references. For example, Hamilton and Melbourne [7] and Thurman [8] have considered the information contained in a single pass of Doppler measurements. Analyses have been extended to several days of data in a number of reports (e.g., [9–11]). However, most of these analyses have considered only data noise and, in some cases, station-location errors. The analysis and computational procedures described here are based on that previous work, but incorporate a number of improvements. A better approximation has been used for the propagation of observables from observation times to the reference epoch. Some terms that have been neglected in the past have been included. Effects of the errors in calibration of the static troposphere, the ionosphere, and the station locations all have been considered simultaneously, with special attention paid to the accuracy of the troposphere and ionosphere models. Finally, the methodology includes the ability to use different Doppler data-weighting functions in order to enable investigation of the improvement in orbit-determination accuracy that might be achieved by using different weighting schemes.

II. Summary of Least-Squares Error Covariance Analysis

The description of least-squares covariance analysis is kept to a minimum here; the reader should consult other references (e.g., [7,8,12]) for more explanation. Consider the range-rate $\dot{\rho}_i$ associated with the ith Doppler measurement. This measurement is modeled as a function of the epoch trajectory $\vec{r}_0$, the measurement time t_i, and the random measurement error n_i, as follows:

$$\dot{\rho}_i = f(\vec{r}_0, t_i) + n_i \tag{1}$$

In a linearized model, measurement residuals $\Delta\dot{\rho}_i$ can be related to perturbations $\Delta\vec{r}_0$ in the trajectory by

$$\Delta\dot{\rho}_i \approx \frac{\partial\dot{\rho}_i}{\partial\vec{r}_0}\,\Delta\vec{r}_0 + n_i \tag{2}$$

The accumulated information matrix, J, for a set of N independent measurements of $\dot{\rho}_i$ with individual weights w_i is

$$J = \sum_{i=1}^{N} w_i\,(\partial\dot{\rho}_i/\partial\vec{r}_0)^T\,(\partial\dot{\rho}_i/\partial\vec{r}_0) \tag{3}$$

If each data point were weighted equally according to an estimate of the variance ${\sigma_D}^2$ of the Doppler measurement, w_i would be replaced by ${\sigma_D}^{-2}$, which could be taken outside the summation. However, since a primary goal of this investigation is to study the effect of a variety of data-weighting schemes, the more general formulation of Eq. (3) will be maintained.

Equation (3) holds for points within a continuous tracking pass as well as for points acquired over several tracking passes. If it is assumed that no a priori information is available, the error covariance matrix Λ_2 is the inverse of the information matrix:

$$\Lambda_2 = J^{-1} \tag{4}$$

III. Partial Derivatives and the Computed Doppler Error Covariance

Consider the case of a spacecraft whose right ascension and declination are denoted by (α, δ), viewed from a tracking station whose cylindrical coordinates with respect to the Earth's center are (r_s,λ_s,z_s). The station-spacecraft tracking geometry is shown in Fig. 1. The range-rate for the spacecraft, $\dot{\rho}$, which can be related directly to the measured Doppler shift, is given approximately by [10]

$$\dot{\rho} \approx \dot{r} - z_s\dot{\delta}\cos\delta + r_s(\dot{\varphi}-\dot{\alpha})\cos\delta\sin(\varphi-\alpha) + r_s\dot{\delta}\sin\delta\cos(\varphi-\alpha) \tag{5}$$

In Eq. (5), r is the spacecraft distance from the center of the Earth, φ (Local Sidereal Time) is the angle between the station meridian and the vernal equinox, and time derivatives are indicated by dots above the variables. The quantity $(\varphi - \alpha)$ is the hour angle of the spacecraft, measured west from the local meridian. The partial derivatives of the range-rate with respect to the six-parameter state vector $\vec{r} = (r,\delta,\alpha,\dot{r},\dot{\delta},\dot{\alpha})$ are given by

$$A_1 \equiv \begin{pmatrix} \partial\dot{\rho}/\partial r \\ \partial\dot{\rho}/\partial\delta \\ \partial\dot{\rho}/\partial\alpha \\ \partial\dot{\rho}/\partial\dot{r} \\ \partial\dot{\rho}/\partial\dot{\delta} \\ \partial\dot{\rho}/\partial\dot{\alpha} \end{pmatrix} = \begin{pmatrix} 0 \\ z_s\dot{\delta}\sin\delta - r_s(\dot{\varphi}-\dot{\alpha})\sin\delta\sin(\varphi-\alpha) + r_s\dot{\delta}\cos\delta\cos(\varphi-\alpha) \\ -r_s(\dot{\varphi}-\dot{\alpha})\cos\delta\cos(\varphi-\alpha) + r_s\dot{\delta}\sin\delta\sin(\varphi-\alpha) \\ 1 \\ -z_s\cos\delta + r_s\sin\delta\cos(\varphi-\alpha) \\ -r_s\cos\delta\sin(\varphi-\alpha) \end{pmatrix} \tag{6}$$

To relate changes in the measured Doppler frequency to changes in the spacecraft state vector $\vec{r}_0$ at some reference epoch t_0, one must find the spacecraft state transition matrix, consisting of the partial derivatives of the state vector $\vec{r}$ with respect to the epoch state vector $\vec{r}_0 = (r_0,\delta_0,\alpha_0,\dot{r}_0,\dot{\delta}_0,\dot{\alpha}_0)$. These partial derivatives constitute a 6×6 matrix A_2 that is a function of the geometry at the reference time and the interval that has passed since that reference time. Formally, the matrix A_2 is expressed as $\partial\vec{r}/\partial\vec{r}_0$. The most common method of deriving this matrix analytically (e.g., [9]) is to linearize all six components of the state vector in time t as follows:

$$\left.\begin{aligned} r &= r_0 + \dot{r}_0 t \\ \delta &= \delta_0 + \dot{\delta}_0 t \\ \alpha &= \alpha_0 + \dot{\alpha}_0 t \\ \dot{r} &= \dot{r}_0 + \ddot{r}_0 t \\ \dot{\delta} &= \dot{\delta}_0 + \ddot{\delta}_0 t \\ \dot{\alpha} &= \dot{\alpha}_0 + \ddot{\alpha}_0 t \end{aligned}\right\} \tag{7}$$

The acceleration terms $\ddot{r}_0$, $\ddot{\delta}_0$, and $\ddot{\alpha}_0$ in Eq. (7) can be expressed as functions of $\vec{r}_0$, thereby enabling a determination of all the relevant partial derivatives. The effects of gravitational acceleration due to the Sun are included in the computation of the partials. The gravitational effects of other bodies have been neglected, so the analysis is useful only for the interplanetary cruise portion of a trajectory, not for the planetary approach/encounter phase.

Formulas for the entries in the matrix A_2 have been derived in [8] and [10]. Occasional sign errors occur in the literature; correct expressions for these partials are given in the Appendix. The formulation here remains cast in terms of the state vector of the spacecraft instead of the coefficients (a,b,c,d,e,f) defined in [6] and [10] to be functions of the six parameters in the state vector.

Most previous covariance analyses (e.g., [9]) employed an A_2 matrix whose terms were functions only of the state vector $\vec{r}_0$ at the epoch time and the time interval since that epoch time. Such a formulation is a good approximation for multiple passes to the extent that the spacecraft motion fits the linear model over the entire data arc.

A more accurate representation of the partial derivatives indicated in Eq. (3) can be obtained by using a piecewise-linear approximation. For each pass, an epoch time is chosen to be the time of spacecraft transit *during that pass.* A linear formulation similar to Eqs. (7) then is used to relate the state vector at any time during a pass to an epoch state vector for the same pass, using the parameter values for the epoch time of the given pass, *not* those for the epoch time of the first pass. Multiplication by the mapping matrices relating each day to the previous day, with the appropriate epoch state vector used for each one-day step in the propagation, provides the mapping matrix to the reference epoch. Hence, the continuously curving spacecraft trajectory is approximated by a series of (six-dimensional) straight lines of different slope rather than by a single straight line.

Mathematically, let the matrix of partials of the state vector for pass j at time t with respect to the epoch state vector at the midpoint of pass j be denoted by $M_j(t)$. This matrix has the same entries as the matrix A_2 (results given in the Appendix), except that $\vec{r}_0$ is replaced by $\vec{r}_{j,0}$, the spacecraft state vector at the transit time for pass j, and the time t is referred to the reference time for pass j, not to the first pass. To relate measurements at time t during pass j to the epoch state vector on day 1, the matrix A_2 should be replaced as follows:

$$A_2 \rightarrow B_2(t) = M_j(t) A_j^{j-1} A_{j-1}^{j-2} \cdots A_3^2 A_2^1$$

$$= M_j(t) \prod_{m=2}^{j} A_{j+2-m}^{j+1-m} \qquad (8)$$

The matrix A_j^{j-1} represents the mapping matrix from the midpoint of pass j to the midpoint of pass $j-1$. Computation of A_j^{j-1} is similar to the computation of the matrix A_2. The straightforward method is to use a linearization process similar to that of Eqs. (7):

$$\left.\begin{aligned} r_{j,0} &= r_{j-1,0} + \tau \dot{r}_{j-1,0} \\ \delta_{j,0} &= \delta_{j-1,0} + \tau \dot{\delta}_{j-1,0} \\ \alpha_{j,0} &= \alpha_{j-1,0} + \tau \dot{\alpha}_{j-1,0} \\ \dot{r}_{j,0} &= \dot{r}_{j-1,0} + \tau \ddot{r}_{j-1,0} \\ \dot{\delta}_{j,0} &= \dot{\delta}_{j-1,0} + \tau \ddot{\delta}_{j-1,0} \\ \dot{\alpha}_{j,0} &= \dot{\alpha}_{j-1,0} + \tau \ddot{\alpha}_{j-1,0} \end{aligned}\right\} \qquad (9)$$

In Eqs. (9), $\vec{r}_{j,0}$ is the state vector of the spacecraft at the transit time for pass j, $\vec{r}_{j-1,0}$ is the similar state vector for the previous pass, and τ is the time between the two transits. In the simple piecewise-linear approximation, A_j^{j-1} would have entries similar to those for A_2 (see Appendix), except that $\vec{r}_0$ would be replaced by $\vec{r}_{j-1,0}$ and t would be replaced by τ. A slightly better approximation has been used in the analysis described here: The entries of A_j^{j-1} are evaluated at $\vec{r}_{j,j-1} \equiv 0.5(\vec{r}_{j-1,0} + \vec{r}_{j,0})$ instead of at $\vec{r}_{j-1,0}$. Thus, the propagation from the transit time for pass j to the transit time for pass $j-1$ uses the average slope of the six-dimensional state vector over the time period between these two times rather than the slope at either end of the period.

Figure 2 is a schematic of several methods of propagating data to the reference time; the curvature of a trajectory over 10 days (i.e., the acceleration) has been exaggerated to highlight the differences. If the actual evolution of a spacecraft state vector is represented by the lower quadratic curve D, the propagation of a state vector found for day 10 to the reference time on day 1 can be represented by three different approximations to the slope of that curve. The horizontal line (labelled A) is the result of using the slope on day 1 to estimate the state vector that would be found for day 1 by propagating back in time from the state vector actually observed on day 10; this is

roughly equivalent to propagating observations from day 10 to the reference time on day 1, using only the epoch state vector of day 1 to evaluate the matrix A_2. The uppermost piecewise-linear "trajectory" (labelled B) uses the slope on day $j-1$ to propagate the trajectory from day j to day $j-1$; it is the same (in principle) as evaluating each matrix A_j^{j-1} at the point $\vec{r}_{j-1,0}$ (namely, the spacecraft state vector at the midpoint of pass $j-1$) and performing the calculation indicated by Eq. (8). Another piecewise-linear approximation (labelled C), virtually indistinguishable from the actual quadratic trajectory (labelled D) in Fig. 2, is equivalent to evaluating each A_j^{j-1} at $\vec{r}_{j,j-1}$ (defined above) and performing the multiplications in Eq. (8). Clearly, the piecewise-linear approximation described in connection with Eqs. (8) and (9) is the best of the three methods shown, although the degree to which it surpasses the other methods depends on the actual curvature of the spacecraft trajectory over a particular data arc.

The partial derivatives of each Doppler measurement with respect to the epoch state vector now can be determined readily from

$$\frac{\partial \dot{\rho}_i}{\partial \vec{r}_0} = \frac{\partial \dot{\rho}_i}{\partial \vec{r}} B_2(t) \tag{10}$$

where B_2 is evaluated as shown in Eq. (8) and described in the accompanying text. Using Eqs. (3), (4), and (10), the error covariance matrix associated with a weighted least-squares estimate of $\vec{r}_0$ can be calculated.

It often is convenient to express the epoch state error covariance in a Cartesian coordinate frame rather than with spherical coordinates. A particularly useful Cartesian frame is the plane-of-sky coordinate system defined by the spacecraft position at epoch, which is depicted in Fig. 3. The position components r_c, r_δ, and r_α represent small position perturbations in the direction of increasing r, δ, and α coordinate directions relative to the nominal epoch spacecraft position. To make the conversion, it is necessary to compute the matrix A_3 containing the partial derivatives of the Cartesian coordinates at the reference time, $(r_{c,0}, r_{\delta,0}, r_{\alpha,0}, \dot{r}_{c,0}, \dot{r}_{\delta,0}, \dot{r}_{\alpha,0})$, with respect to the spherical coordinates $(r_0, \delta_0, \alpha_0, \dot{r}_0, \dot{\delta}_0, \dot{\alpha}_0)$. Reference [11] gives those derivatives, but contains several errors; correct values for the partials matrix A_3 are given in the Appendix.

It easily can be shown that the plane-of-sky Cartesian covariance matrix, Λ_{pos}, is given by

$$\Lambda_{\text{pos}} = A_3 \Lambda_{\text{sph}} A_3{}^T \tag{11}$$

In Eq. (11), Λ_{sph} is simply the error covariance matrix for the spacecraft spherical coordinates at epoch.

IV. Description of Consider-State Error Covariance Analysis

A. Brief Review of Theory

The error covariance calculation outlined in Sections II and III could be used to predict the orbit-determination error statistics obtained from a series of Doppler measurements if each measurement were affected only by random, uncorrelated errors. However, systematic errors also can be present in the Doppler data due to imperfect calibration of a number of quantities that often are not solved for in the orbit-determination process. The sensitivity of the computed trajectory to these error sources can be estimated by allowing their influence to be "considered" in determining the error statistics associated with the computed trajectory. Obviously, the use of such a procedure results in a suboptimal estimate of the spacecraft trajectory, an estimate that does not minimize the expected value of the mean-squared estimation errors. This subsection reviews briefly the procedures for calculating a "consider" error covariance, while the following subsection describes the particular set of considered parameters included in the current analysis.

A consider-state covariance analysis primarily involves the computation of the partial derivatives of the estimated epoch state vector, $\vec{r}_{0,e}$, with respect to the consider parameters $\vec{y}_c$. The consider parameters are those quantities that are not estimated explicitly in the orbit determination. To perform the computation, the partial derivatives of the Doppler observable $\dot{\rho}$ with respect to the consider parameters $\vec{y}_c$ must be found and then used in combination with the partials of $\dot{\rho}$ with respect to $\vec{r}_0$ to calculate the desired quantities. (Note that $\vec{r}_{0,e}$ is the *estimated* state vector, while $\vec{r}_0$ is the *actual* state vector.) Formally, define the matrix $\partial \vec{r}_{0,e}/\partial \vec{y}_c$ as the sensitivity matrix, denoted as S. A detailed derivation of the sensitivity matrix is given by McReynolds [13]; only the results will be summarized here. The sensitivity matrix can be expressed as a function of the computed covariance, Λ_2, representing the uncertainty in the estimated parameters due to the random measurement errors (the "data noise"), and an additional matrix as follows:

$$\left.\begin{aligned} S &\equiv \partial \vec{r}_{0,e}/\partial \vec{y}_c \\ &= \Lambda_2 \sum_{i=1}^{N} w_i \, (\partial \dot{\rho}_i/\partial \vec{r}_0)^T \, (\partial \dot{\rho}_i/\partial \vec{y}_c) \end{aligned}\right\} \tag{12}$$

Recall that the computed covariance, Λ_2, given in Eq. (4) is just the inverse of the information matrix. Now let the matrix Λ_y represent the error covariance matrix for the consider parameters. The matrix Λ_y is assumed to be diagonal in this analysis, with entries equal to the variances in the knowledge of the individual consider parameters. The statistical uncertainty introduced into the estimated parameters (the spacecraft epoch state vector elements) by the consider parameters, denoted by the covariance matrix Λ_1, is given by

$$\Lambda_1 = S\Lambda_y S^T \tag{13}$$

Finally, the total, or consider, error covariance for the estimated parameters, Λ_3, due to both random measurement errors and the consider parameters, is

$$\Lambda_3 = \Lambda_1 + \Lambda_2 \tag{14}$$

If desired, the error covariance matrix for the spacecraft epoch state vector given in Eq. (14) can be expressed readily in a plane-of-sky Cartesian frame using the mapping formula in Eq. (11).

The formulation given thus far for the consider error covariance is valid only if the weights w_i assigned to the Doppler data are equal to $1/{\sigma_D}^2$. If the weights used are not the inverse of the data noise variance, then the formulas given for Λ_1 and Λ_2 in Eqs. (13) and (4) must be modified. This scenario is of particular interest here, since the following section describes a Doppler weighting technique in which the data weights are *not* equal to the inverse of the data noise variance. This weighting scheme is designed to reduce the sensitivity of Doppler-based trajectory estimates to errors in the calibration of the transmission media and the station locations. For this more general problem, it can be shown[1] that the computed covariance, Λ_2, is

$$\Lambda_2 = (A^T W A)^{-1} A^T W \Lambda_\eta W A (A^T W A)^{-1} \tag{15a}$$

where

$$A = \begin{pmatrix} \partial\dot{\rho}_1/\partial\vec{r}_0 \\ \partial\dot{\rho}_2/\partial\vec{r}_0 \\ \cdot \\ \cdot \\ \partial\dot{\rho}_N/\partial\vec{r}_0 \end{pmatrix} \tag{15b}$$

$$W = \begin{pmatrix} w_1 & 0 & \cdot & \cdot & 0 \\ 0 & w_2 & \cdot & \cdot & 0 \\ \cdot & \cdot & \cdot & \cdot & 0 \\ \cdot & \cdot & \cdot & \cdot & 0 \\ 0 & 0 & \cdot & \cdot & w_N \end{pmatrix} \tag{15c}$$

and

$$\Lambda_\eta = I \cdot {\sigma_D}^2 \tag{15d}$$

For $W = I \cdot {\sigma_D}^{-2}$, Eq. (15a) reduces to $\Lambda_2 = (A^T W A)^{-1}$, as it should. To form the sensitivity matrix in the general case, Eq. (12) still is appropriate, but with the expression in Eq. (15a) used for the computed covariance Λ_2. The formula for the consider error covariance Λ_3, given in Eq. (14), then is unchanged after making the necessary modification to Eq. (12). This general formulation was used in the analysis described herein.

B. Consider Partial Derivatives

The particular analysis described here includes three different consider error sources. These consider parameters are (1) the calibration errors in the wet and dry components of the static zenith tropospheric delay; (2) the calibration errors in the daytime and nighttime ionospheric delay; and (3) the uncertainties in the station location. All delays are expressed in units of length, and fluctuations in the delays are ignored here. Although the uncertainties in universal time and polar motion (UTPM) are not included explicitly, these errors give signatures similar to uncertainties in station location; for instance, an error in universal time is exactly equivalent to an error in station longitude. Therefore, the analysis should give a reasonable picture of the effects of UTPM errors provided that the assumed magnitudes of the station-location errors are large enough to encompass the UTPM errors as well.

The partial derivatives of the Doppler observable with respect to calibration errors in the wet and dry components of the zenith troposphere have been computed by Russell[2] and are reproduced here. Define γ to be the elevation angle, and $\dot{\gamma}$ to be its time derivative. Then, for a single tracking station, the partial derivative with respect to an error $\Delta\rho_{z_W}$ in the calibration of the wet zenith delay is given by

$$\frac{\partial\dot{\rho}}{\partial(\Delta\rho_{z_W})} = 2f(\mathcal{A}_2, \mathcal{B}_2, \gamma, \dot{\gamma}) \tag{16a}$$

[1] R. K. Russell, "The Development of Parameter Estimation," Engineering Note 001-100 (internal document), Jet Propulsion Laboratory, Pasadena, California, January 19, 1987.

[2] R. K. Russell, "Computation of Troposphere Partial Derivatives," JPL Engineering Memorandum 391-277 (internal document), Jet Propulsion Laboratory, Pasadena, California, February 3, 1972.

where

$$f(\mathcal{A},\mathcal{B},\gamma,\dot{\gamma}) = -\dot{\gamma}\left[\sin\gamma + \frac{\mathcal{A}}{\tan\gamma+\mathcal{B}}\right]^{-2} \times \left[\cos\gamma - \frac{\mathcal{A}}{(\sin\gamma+\mathcal{B}\cos\gamma)^2}\right] \quad (16b)$$

The partial with respect to an error $\Delta\rho_{z_D}$ in the calibration of the dry zenith delay is

$$\frac{\partial\dot{\rho}}{\partial(\Delta\rho_{z_D})} = 2f(\mathcal{A}_1,\mathcal{B}_1,\gamma,\dot{\gamma}) \quad (17)$$

where f was defined in Eq. (16b). The constants $\mathcal{A}_1$, $\mathcal{A}_2$, $\mathcal{B}_1$, and $\mathcal{B}_2$ were determined by ray-tracing calculations to be

$$\left.\begin{aligned}\mathcal{A}_1 &= 0.00143\\ \mathcal{A}_2 &= 0.00035\\ \mathcal{B}_1 &= 0.0445\\ \mathcal{B}_2 &= 0.017\end{aligned}\right\} \quad (18)$$

The consider partials that relate to errors in calibration of the ionospheric propagation have been given by Jacobson[3] in terms of the daytime and nighttime "ionospheric coefficients" ($\mathcal{D}$ and $\mathcal{N}$), which essentially represent the delay errors at zenith during the day and night. The expressions for the partial derivatives are

$$\frac{\partial\dot{\rho}}{\partial\mathcal{D}} = -\cos x\frac{d}{dt}(\sec z) - \dot{x}\sin x\sec z \quad (19a)$$

and

$$\frac{\partial\dot{\rho}}{\partial\mathcal{N}} = -\frac{d}{dt}(\sec z) \quad (19b)$$

In Eqs. (19a) and (19b), z is the zenith angle of the spacecraft as seen from the point where the line of sight from the tracking station passes through the mean ionospheric height of 350 km ($z = \sin^{-1}[0.948\cos\gamma]$); x is the minimum of $\pi/2$ and $|2\pi(t-\theta)/P|$, where P is the period of the diurnal variation of the ionosphere (taken to be 32 hours), θ is the phase of that variation (taken to be 14 hours of time), and t is the local time at the subionospheric point. To compute the partials, this time can be written in terms of the station location, the universal time, and the direction to the spacecraft; the interested reader is referred to the work by Jacobson[3] or to [14] for further details.

Making use of Eq. (5) and the fact that for longitudes increasing to the east, $\partial/\partial\lambda_s = \partial/\partial\varphi$ (i.e., moving the station to the east is the same as increasing the local sidereal time), the partial derivatives with respect to the cylindrical station coordinates (r_s,λ_s,z_s) easily are shown to be

$$\left.\begin{aligned}\frac{\partial\dot{\rho}}{\partial r_s} &= (\dot{\varphi}-\dot{\alpha})\cos\delta\sin(\varphi-\alpha) + \dot{\delta}\sin\delta\cos(\varphi-\alpha)\\ \frac{\partial\dot{\rho}}{\partial\lambda_s} &= r_s[(\dot{\varphi}-\dot{\alpha})\cos\delta\cos(\varphi-\alpha) - \dot{\delta}\sin\delta\sin(\varphi-\alpha)]\\ \frac{\partial\dot{\rho}}{\partial z_s} &= -\dot{\delta}\cos\delta\end{aligned}\right\} \quad (20)$$

In Eq. (20), the partials with respect to r_s and z_s are in units of velocity divided by distance, while the partial with respect to λ_s is in units of velocity per radian. To convert the partial with respect to λ_s to the same units as the other partials, the partial derivative given in Eq. (20) should be divided by r_s.

V. Weighting Functions

The consider covariance analysis procedure described above carried the weighting factor w_i for each Doppler measurement; w_i nominally is chosen to be $1/{\sigma_D}^2$ in conventional least-squares estimation. However, Doppler data can be affected by large consider errors at low elevations because of the effects of the ionosphere and the troposphere on signal propagation, as well as the elevation-independent effects of uncertain calibration of station locations and Earth-orientation parameters. In many cases, the inclusion of low-elevation data actually has resulted in larger uncertainties in operational navigation than have been obtained by discarding those data. Therefore, one common approach to this problem has been to discard all data below a specified elevation angle. A second approach has been to deweight all data uniformly, which

[3] R. A. Jacobson, "Troposphere and Ionosphere Delay Models in ATHENA," JPL Engineering Memorandum 314-290 (internal document), Jet Propulsion Laboratory, Pasadena, California, November 16, 1982.

has the effect of making the high-elevation data "as bad" as the low-elevation data and is not likely to give the best trajectory determination. A third possibility, considered below, is to deweight the low-elevation data according to some function appropriate to minimize troposphere and/or ionosphere effects on the estimated trajectory. (This deweighting might be accompanied by imposition of an elevation cutoff.) The single most important motivation for constructing the consider analysis methodology described in this article was to make a systematic, quantitative investigation of various weighting functions that would lead to recommendations regarding appropriate methods of weighting 8.4-GHz and 32-GHz Doppler data.

The consider analysis described here has been implemented in a computer program that includes a weighting function of the following form:

$$\left.\begin{aligned} w_i &= \left[\sigma_D{}^2 + \left(\frac{\sigma_e}{(\sin\gamma)^q}\right)^2\right]^{-1}, \quad \gamma > \gamma_{\min} \\ &= 0, \qquad\qquad\qquad\qquad \gamma < \gamma_{\min} \end{aligned}\right\} \quad (21)$$

This weighting function was postulated because it resembles, in an approximate form, the behavior of the troposphere partial derivatives given by Eqs. (16) and (17). As before, γ is the elevation angle of the spacecraft as viewed from the tracking station. The elevation-dependent part of the weighting function has the form $(\sigma_e/\sin^q\gamma)^2$, where q is a selectable exponent and σ_e is a selectable weighting factor. The assumed Doppler data noise variance is $\sigma_D{}^2$, and all data at elevations below $\gamma_{\min}$ are discarded (this elevation cutoff also is user-selectable). Note that with this form of weighting, the data analyst has the option of adjusting the weighting function in several ways. Data can be deweighted uniformly by increasing the value of σ_D and choosing $\sigma_e = 0$. Data can be deweighted as a function of elevation angle by appropriate selection of σ_e and q. Finally, $\gamma_{\min}$ can be varied to change the cutoff angle.

Figures 4(a) and 4(b) are plots of the partial derivatives given by Eqs. (16)–(19) as functions of the elevation angle γ. These plots are for a segment of the Mars Observer trajectory, whose state vector is given in Table 1. Tracking from the Goldstone Deep Space Network complex (latitude of about 35.2 deg) is assumed. Note that the troposphere partials are dominant at the low elevation angles, reaching values about 40 times greater than the maximum ionosphere partials in this particular case. For observations at 8.4 GHz, the uncertainties in the coefficients $\mathcal{D}$ and $\mathcal{N}$ are comparable to the values of $\Delta\rho_{z_D}$ and $\Delta\rho_{z_W}$, implying that the troposphere calibration error will dominate the effects of the ionosphere calibration error in the Doppler data. At 2.3 GHz, $\mathcal{D}$ and $\mathcal{N}$ are larger by a factor of ~ 13 and can be much more important.

Figure 5 shows the Doppler data weights as a function of elevation angle for several different values of the variable parameters in Eq. (21); of course, the weights at the lower elevation points can be set to zero arbitrarily by making a choice of $\gamma_{\min}$. In this figure, an arbitrary value of unity is assigned to the Doppler data noise (i.e., $\sigma_D \equiv 1$). Values of 1, 2, and 3 are used for q, while σ_e is set equal to either σ_D or 0.5 σ_D. For comparison, Fig. 6 is a plot of the *inverse* of the troposphere partial derivatives. If the troposphere were the *only* contributing calibration error and dominated the data noise in determining the Doppler error, the ideal weighting function would have a shape similar to the curves in Fig. 6. A comparison of Figs. 5 and 6 implies that the weighting functions with values of $q = 2$ or $q = 3$ may be more appropriate for Doppler data whose errors are dominated by errors in the troposphere calibration.

Note that the shapes of the weighting functions in Fig. 5 already lead to an interesting conclusion. When the weighting function is a strong function of elevation angle (i.e., $q \approx 3$), the choice of elevation cutoffs should make very little difference in the final results of the analysis. This is because, for the larger values of q, the low-elevation data already are downweighted so much that they have little effect on the orbit determination; they effectively have been discarded even before the elevation limit is applied. The specification of an elevation cutoff would be more important if the ratio of σ_e to σ_D in Eq. (21) were much smaller than the values used in generating the plot in Fig. 5.

VI. Accuracy Over Long Data Arcs

It was mentioned previously that the trajectory representation developed herein breaks down for long data arcs, but the maximum length of time for which the approximations are valid was not specified. However, it is possible to make a rough estimate of the longest data arcs that might be investigated using the formalism described above. This estimate has been made by considering the accuracy of the linear approximation given by Eqs. (7) and the accuracy of the piecewise-linear approximation described by Eqs. (8) and (9) and in the surrounding discussion.

A more accurate system of equations would include terms that are quadratic in time:

$$\left.\begin{aligned} r &= r_0 + \dot{r}_0 t + \ddot{r}_0 t^2/2 \\ \delta &= \delta_0 + \dot{\delta}_0 t + \ddot{\delta}_0 t^2/2 \\ \alpha &= \alpha_0 + \dot{\alpha}_0 t + \ddot{\alpha}_0 t^2/2 \\ \dot{r} &= \dot{r}_0 + \ddot{r}_0 t + t^2(\partial^3 r_0/\partial t^3)/2 \\ \dot{\delta} &= \dot{\delta}_0 + \ddot{\delta}_0 t + t^2(\partial^3 \delta_0/\partial t^3)/2 \\ \dot{\alpha} &= \dot{\alpha}_0 + \ddot{\alpha}_0 t + t^2(\partial^3 \alpha_0/\partial t^3)/2 \end{aligned}\right\} \quad (22)$$

As an example, consider the partial derivative $\partial r/\partial r_0$. In the linear theory, this partial derivative is found as follows:

$$\frac{\partial r}{\partial r_0} = 1 + t\frac{\partial \dot{r}_0}{\partial r_0} = 1 \quad (23a)$$

since $(\partial \dot{r}_0/\partial r_0) = 0$. Keeping the quadratic time terms as in Eq. (22), letting $\ddot{r}_g$ be the line-of-sight acceleration due to the Sun's gravitational field, and using the result from [10] that

$$\ddot{r}_0 = r_0(\dot{\delta}_0^2 + \dot{\alpha}_0^2 \cos^2 \delta_0) + \ddot{r}_g \quad (23b)$$

this partial derivative is

$$\left.\begin{aligned} \frac{\partial r}{\partial r_0} &= 1 + t\frac{\partial \dot{r}_0}{\partial r_0} + \frac{t^2}{2}\frac{\partial \ddot{r}_0}{\partial r_0} \\ &= 1 + \frac{t^2}{2}\left(\dot{\delta}_0^2 + \dot{\alpha}_0^2 \cos^2 \delta_0 + \frac{\partial \ddot{r}_g}{\partial r_0}\right) \\ &= 1 + \frac{t^2}{2} \\ &\quad \times \left(\dot{\delta}_0^2 + \dot{\alpha}_0^2 \cos^2 \delta_0 + \frac{\mu}{{r_{p,0}}^3}\left[2 - 3\sin^2 \psi_0\right]\right) \end{aligned}\right\} \quad (23c)$$

In the above equation, μ is the universal gravitational constant multiplied by the mass of the Sun, $r_{p,0}$ is the Sun–spacecraft distance, and ψ_0 is the Earth–spacecraft–Sun angle. The value of $\partial \ddot{r}_g/\partial r_0$ has been taken from [10]. As an example, a segment of the planned Mars Observer trajectory on July 22, 1993 was taken, with epoch state parameters as shown in Table 1. Using the appropriate numbers, Eq. (23c) becomes

$$\frac{\partial r}{\partial r_0} = 1 + 2.6 \times 10^{-14} t^2 \quad (24)$$

where t is given in seconds. Thus, the linear approximation used in the standard derivation of the state transition matrix A_2 would have a fractional error of $2.6 \times 10^{-14} t^2$. The partial derivative would be accurate at the 1-percent level only if t were smaller than 6.2×10^5 seconds, or about 7 days. For 10-percent accuracy in the partial, t could be no greater than 23 days.

The piecewise-linear approximation to the trajectory includes the bulk of the effect of the quadratic terms. Considering the transition matrix connecting day 2 to day 1, A_2^1, the maximum value of t that would be used in Eq. (24) would be about a day, or 8.6×10^4 seconds. The connection from day 3 to day 1 is based on two values of the partial derivative, which differ because of the effects of the quadratic terms included in a piecewise-linear manner. Thus, the fractional error for each day's pass would be indicated by Eq. (24), but the total fractional error over an n-day data arc is approximately

$$\left.\begin{aligned} f_n &\approx \left(1 + 2.6 \times 10^{-14} T^2\right)^n - 1 \\ &\approx 2.6 \times 10^{-14} n T^2 \end{aligned}\right\} \quad (25a)$$

instead of

$$\left.\begin{aligned} f_n &\approx \left[1 + 2.6 \times 10^{-14} (nT)^2\right] - 1 \\ &= 2.6 \times 10^{-14} n^2 T^2 \end{aligned}\right\} \quad (25b)$$

where T is the length of a day in seconds. These two equations differ in only one respect, their dependence on the number of days n in the data arc. For $n = 7$, Eq. (25b) predicts a fractional error of 0.95 percent for the linear approximation, while Eq. (25a) predicts a fractional error of 0.14 percent for the piecewise-linear approximation. For a month-long data arc, $n = 30$, the fractional error for the linear approximation would be about 17 percent, while that for the piecewise-linear approximation would be only 0.6 percent! In fact, even this result is an overestimate of the inaccuracy of the piecewise-linear approximation used in the analysis developed in this article. When the transition state matrix between passes j and $j-1$ is evaluated for the state vector $\vec{r}_{j,j-1}$ at the midpoint between the two

passes, a more appropriate value of T used in Eq. (25a) would be half the length of the day rather than the full length of a day. In any case, it is clear that the length of the data arc that can be considered is substantially longer than that possible for the simple linear approximation.

Provided that calculations of the neglected terms in other partial derivatives give results similar to those described above, for the particular sample trajectory considered here, the piecewise-linear approximation represented by Eq. (8) should be quite good for data arcs longer than a month. The approximation would hold for a longer period cruise trajectory in the outer solar system, say at the distance of Jupiter, since the numerical coefficient of T^2 in Eq. (25a) would be considerably smaller. For a trajectory near Venus, the gravitational acceleration due to the Sun would be larger, reducing the accuracy of the linear approximation. In that case, the advantage of the piecewise-linear approximation would be even more pronounced. It is possible to get arbitrarily close to the true model of state-vector evolution by breaking the data arc into more pieces, but the above estimate shows that the simple piecewise-linear approximation that is used should be quite good for most circumstances.

VII. Summary

This article has described an error covariance analysis methodology for Doppler measurements that can be used to predict errors in the estimated state vector of an interplanetary spacecraft in the cruise portion of its trajectory. The analysis and associated computer program improve on previously published analyses in several ways: (1) The effects of imperfect calibration of the static troposphere, the static ionosphere, and the station location are all considered simultaneously; (2) the spacecraft state transition matrix is modelled more accurately, using a piecewise-linear approximation to represent the evolution of the spacecraft trajectory; and (3) the Doppler data can be weighted according to elevation angle in an attempt to minimize the covariance associated with determination of the spacecraft trajectory. The first and second "improvements" or better representations also are available in comprehensive software such as the JPL Orbit Determination Program [15], but the limited focus of the analysis method described in this article makes it preferable for investigation of a large number of possible cases of data weighting in a short period of time.

The analysis method described in this article is useful for estimating the errors in trajectory determination for data arcs longer than a month in the case of a spacecraft more than 1 AU from the Sun and far from the gravitational influence of any planets. In the case of spacecraft in the outer solar system (e.g., Voyager and Galileo), the reduced gravitational effect of the Sun and the smaller angular velocities of the spacecraft should enable use of this formulation for a considerably longer data arc; the period of validity needs to be evaluated on a case-by-case basis. It is likely that the accumulated effects of nongravitational, unmodelled accelerations would lead to greater errors than those caused by the piecewise-linear inclusion of the quadratic terms due to known gravitational effects.

Acknowledgments

The authors thank Jim McDanell for an enlightening discussion on modification of the consider error covariance for arbitrary data weighting, Stuart Demczak for supplying the state vector for the Mars Observer trajectory segment, and Bob Jacobson for careful review of a draft of this article.

References

[1] J. K. Miller and K. H. Rourke, "The Application of Differential VLBI to Planetary Approach Orbit Determination," *Deep Space Network Progress Report,* vol. May–June 1977, Jet Propulsion Laboratory, Pasadena, California, pp. 84–90, August 15, 1977.

[2] J. E. Riedel, W. M. Owen, Jr., J. A. Stuve, S. P. Synnott, and R. M. Vaughan, "Optical Navigation During the Voyager Neptune Encounter," paper AIAA-90-2877, AIAA/AAS Astrodynamics Conference, Portland, Oregon, August 20–22, 1990.

[3] S. W. Thurman, "Deep-Space Navigation With Differenced Data Types, Part I: Differenced Range Information Content," *TDA Progress Report 42-103,* vol. July–September 1990, Jet Propulsion Laboratory, Pasadena, California, pp. 47–60, November 15, 1990.

[4] S. W. Thurman, "Deep-Space Navigation with Differenced Data Types, Part II: Differenced Doppler Information Content," *TDA Progress Report 42-103,* vol. July–September 1990, Jet Propulsion Laboratory, Pasadena, California, pp. 61–69, November 15, 1990.

[5] C. D. Edwards, "Angular Navigation on Short Baselines Using Phase Delay Interferometry," *IEEE Transactions on Instrumentation and Measurement,* vol. 38, no. 2, pp. 665–667, April 1989.

[6] W. M. Folkner, D. B. Engelhardt, J. S. Border, and N. A. Mottinger, "Orbit Determination for Magellan and Pioneer 12 Using Same-Beam Interferometry," paper AAS 91-393, AIAA/AAS Astrodynamics Conference, Durango, Colorado, August 19–22, 1991.

[7] T. W. Hamilton and W. G. Melbourne, "Information Content of a Single Pass of Doppler Data from a Distant Spacecraft," *JPL Space Programs Summary,* no. 37-39. vol. III, Jet Propulsion Laboratory, Pasadena, California, pp. 18–23, March–April 1966.

[8] S. W. Thurman, "Comparison of Earth-Based Radio Metric Data Strategies for Deep Space Navigation," paper AIAA 90-2908, AIAA/AAS Astrodynamics Conference, Portland, Oregon, August 22, 1990.

[9] D. W. Curkendall and S. R. McReynolds, "A Simplified Approach for Determining the Information Content of Radio Tracking Data," *Journal of Spacecraft and Rockets*, vol. 6, no. 5, pp. 520–525, May 1969.

[10] V. J. Ondrasik and D. W. Curkendall, "A First-Order Theory for Use in Investigating the Information Content Contained in a Few Days of Radio Tracking Data," *Deep Space Network Progress Report*, JPL Technical Report 32-1526, vol. III, Jet Propulsion Laboratory, Pasadena, California, pp. 77–93, June 15, 1971.

[11] D. W. Curkendall, "Problems in Estimation Theory with Applications to Orbit Determination," Ph.D. thesis, Los Angeles: University of California at Los Angeles, 1971.

[12] P. R. Escobal, *Methods of Orbit Determination*, 2nd ed., Malabar, Florida: Robert E. Krieger Publishing Company, pp. 435–450, 1976.

[13] S. R. McReynolds, "The Sensitivity Matrix Method for Orbit Determination Error Analysis, With Application to a Mars Orbiter," *JPL Space Programs Sum-*

mary, no. 37-56, vol. II, January–February 1969, Jet Propulsion Laboratory, Pasadena, California, pp. 85–87, March 31, 1969.

[14] J. A. Klobuchar, *A First Order, World-Wide, Ionospheric Time-Delay Algorithm*, Document AFCRL-TR-75-0502, Hanscom AFB, Massachusetts: Air Force Cambridge Research Laboratories, September 25, 1975.

[15] T. D. Moyer, *Mathematical Formulation of the Double-Precision Orbit Determination Program (DPODP)*, Technical Report 32-1527, Jet Propulsion Laboratory, Pasadena, California, May 15, 1971.

Table 1. Initial state vector for a segment of Mars Observer trajectory.

Parameter	Value
Year	1993
Day of year	203 (22 July)
Distance, km	3.1573×10^{8}
Right ascension (α), deg	169.0252
Declination (δ), deg	5.1308
Radial velocity, km/sec	11.5770
$d\alpha/dt$, deg/sec	6.2454×10^{-6}
$d\delta/dt$, deg/sec	-2.5866×10^{-6}

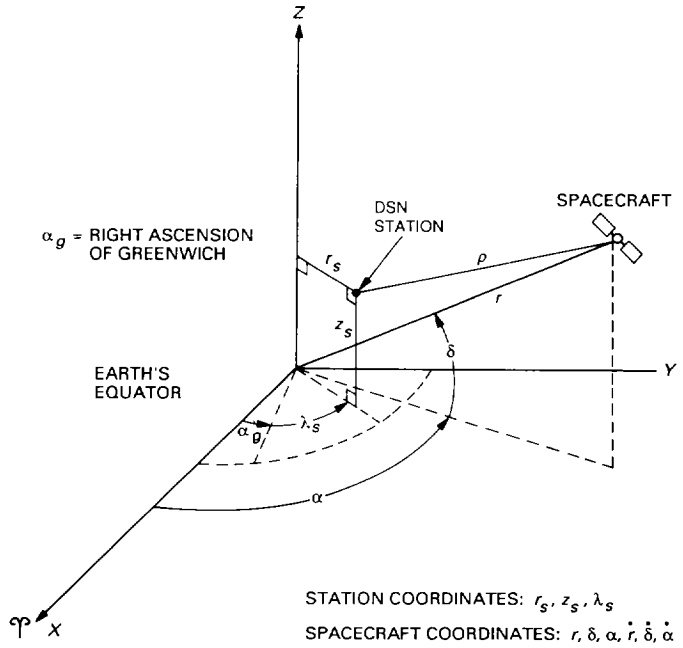

Fig. 1. Station–spacecraft tracking geometry.

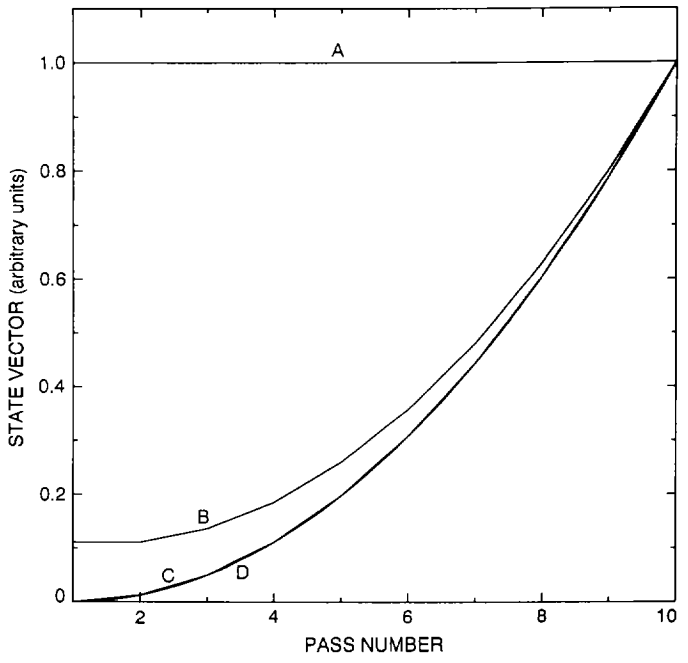

Fig. 2. The effect of different methods of computing a spacecraft state transition matrix.

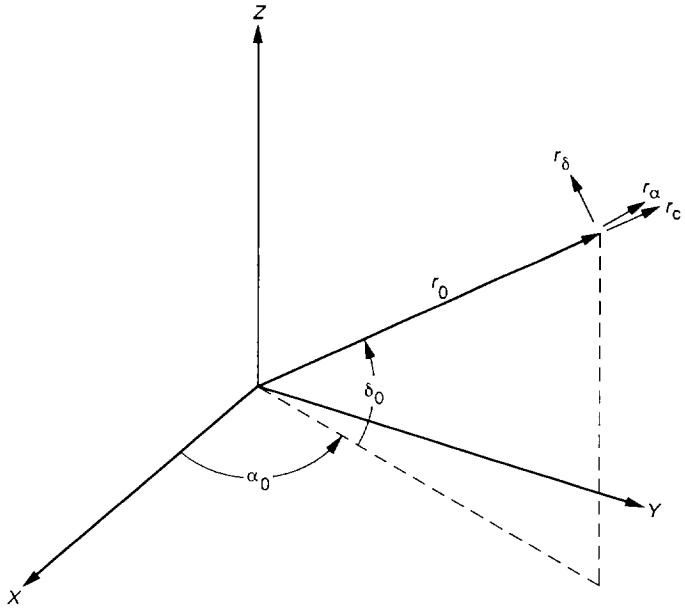

Fig. 3. Geocentric plane-of-sky Cartesian coordinate system.

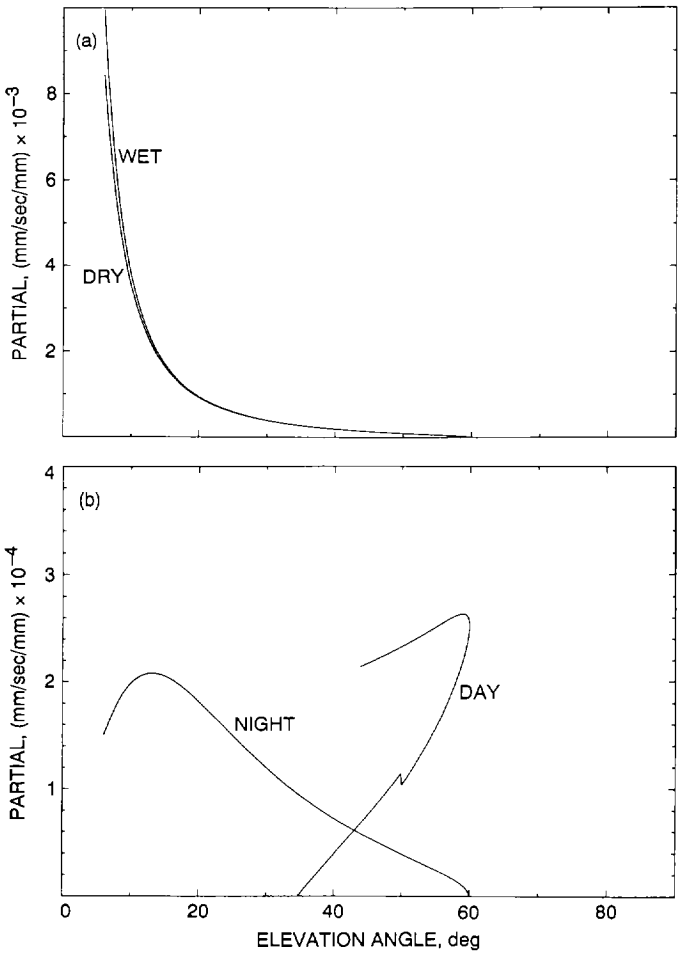

Fig. 4. Partial derivatives of the Doppler error with respect to the calibration errors in the troposphere and ionosphere delays plotted against elevation angle: (a) partials of the Doppler observable with respect to wet and dry zenith-troposphere calibration errors, and (b) partials of the Doppler observable with respect to daytime and nighttime ionosphere coefficients.

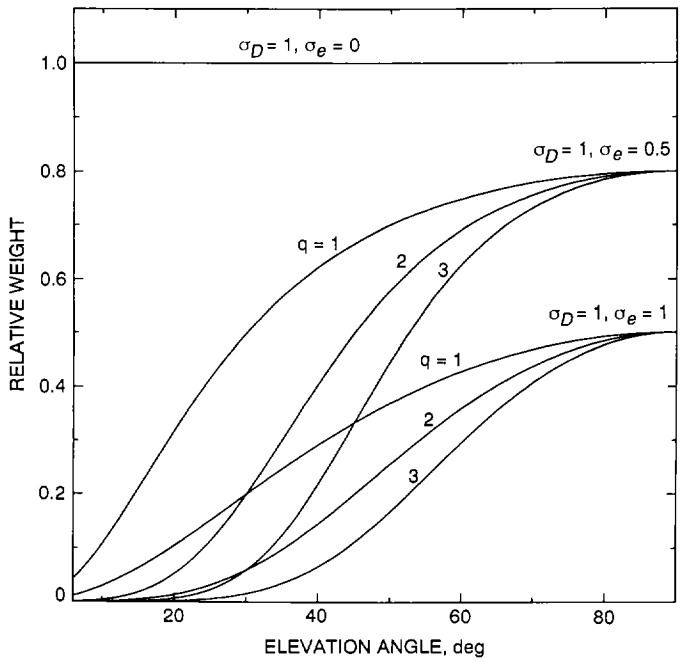

Fig. 5. The weighting function given by Eq. (21) for a cutoff elevation of 6 deg: Three different values of the exponent q are included for each family.

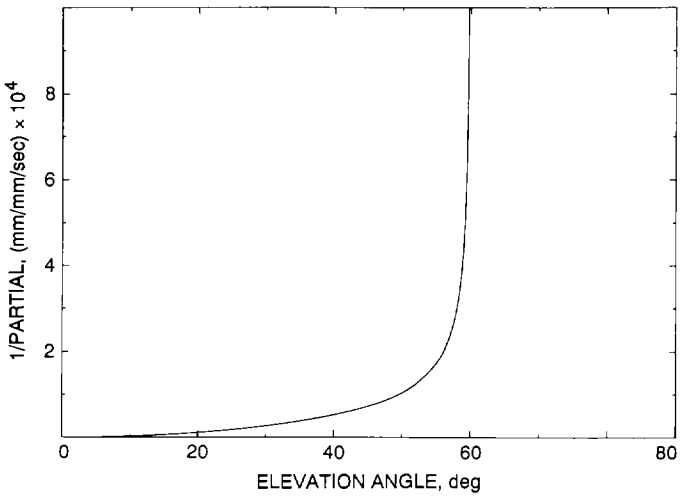

Fig. 6. Inverse of the partials of the Doppler error with respect to errors in the calibration of the zenith troposphere delay. Plots for wet and dry components overlap. The plot goes to infinity at transit, where $\dot{\gamma}$ goes to zero in Eq. (16b).

Appendix

Summary of Partial Derivatives

This appendix gives (without derivation) the partial derivatives in the 6 × 6 matrices A_2 and A_3 described in Section III. A_2 is the matrix of partials of the state vector $\vec{r}$ at an arbitrary time t with respect to the state vector $\vec{r}_0$ at the epoch time for the same pass. To find the matrix of partials relating the state vector at the epoch time on day j to that at the epoch time on day $j-1$, denoted A_j^{j-1} in Section III, $\vec{r}_0$ should be replaced by $\vec{r}_{j,j-1}$ and t by τ, as described following Eq. (9).

The matrix A_2 is defined as follows:

$$A_2 = \begin{pmatrix} \frac{\partial r}{\partial r_0} & \frac{\partial r}{\partial \delta_0} & \frac{\partial r}{\partial \alpha_0} & \frac{\partial r}{\partial \dot{r}_0} & \frac{\partial r}{\partial \dot{\delta}_0} & \frac{\partial r}{\partial \dot{\alpha}_0} \\ \frac{\partial \delta}{\partial r_0} & \frac{\partial \delta}{\partial \delta_0} & \frac{\partial \delta}{\partial \alpha_0} & \frac{\partial \delta}{\partial \dot{r}_0} & \frac{\partial \delta}{\partial \dot{\delta}_0} & \frac{\partial \delta}{\partial \dot{\alpha}_0} \\ \frac{\partial \alpha}{\partial r_0} & \frac{\partial \alpha}{\partial \delta_0} & \frac{\partial \alpha}{\partial \alpha_0} & \frac{\partial \alpha}{\partial \dot{r}_0} & \frac{\partial \alpha}{\partial \dot{\delta}_0} & \frac{\partial \alpha}{\partial \dot{\alpha}_0} \\ \frac{\partial \dot{r}}{\partial r_0} & \frac{\partial \dot{r}}{\partial \delta_0} & \frac{\partial \dot{r}}{\partial \alpha_0} & \frac{\partial \dot{r}}{\partial \dot{r}_0} & \frac{\partial \dot{r}}{\partial \dot{\delta}_0} & \frac{\partial \dot{r}}{\partial \dot{\alpha}_0} \\ \frac{\partial \dot{\delta}}{\partial r_0} & \frac{\partial \dot{\delta}}{\partial \delta_0} & \frac{\partial \dot{\delta}}{\partial \alpha_0} & \frac{\partial \dot{\delta}}{\partial \dot{r}_0} & \frac{\partial \dot{\delta}}{\partial \dot{\delta}_0} & \frac{\partial \dot{\delta}}{\partial \dot{\alpha}_0} \\ \frac{\partial \dot{\alpha}}{\partial r_0} & \frac{\partial \dot{\alpha}}{\partial \delta_0} & \frac{\partial \dot{\alpha}}{\partial \alpha_0} & \frac{\partial \dot{\alpha}}{\partial \dot{r}_0} & \frac{\partial \dot{\alpha}}{\partial \dot{\delta}_0} & \frac{\partial \dot{\alpha}}{\partial \dot{\alpha}_0} \end{pmatrix} \quad \text{(A-1)}$$

A number of definitions must be made to write the partial derivatives in a reasonably compact form; the definitions made here largely follow those in [10], and all variables are assumed to be evaluated at the reference (or epoch) time indicated by the subscript "0." Let the right ascension and declination of the Sun be denoted by $\alpha_{s,0}$ and $\delta_{s,0}$, respectively. Denote the Earth–Sun distance by $r_{e,0}$ and the Earth–spacecraft distance by $r_{p,0}$. The Sun–Earth–spacecraft angle is χ_0, where

$$\cos\chi_0 = \cos\delta_0 \cos\delta_{s,0} \cos(\alpha_0 - \alpha_{s,0}) + \sin\delta_0 \sin\delta_{s,0} \quad \text{(A-2)}$$

The Earth–spacecraft–Sun angle ψ_0 is found from

$$\sin\psi_0 = r_{e,0} \sin\chi_0 / r_{p,0} \quad \text{(A-3)}$$

where

$$r_{p,0} = \left[r_0^2 + r_{e,0}^2 - 2 r_0 r_{e,0} \cos\chi_0\right]^{1/2} \quad \text{(A-4)}$$

The angle σ_0 is given by

$$\cos\sigma_0 = -\sin\delta_0 \cos\delta_{s,0} \cos(\alpha_0 - \alpha_{s,0}) + \cos\delta_0 \sin\delta_{s,0} \quad \text{(A-5)}$$

Reference [10] gives the gravitational accelerations of the spacecraft in the radial, declination, and right-ascension directions $(\ddot{r}_g, \ddot{\delta}_g, \ddot{\alpha}_g)$. If μ is the product of the universal gravitational constant and the mass of the Sun, those accelerations are

$$\ddot{r}_g = \frac{-\mu r_0}{r_{p,0}^3} + \mu r_{e,0} \cos\chi_0 \left(\frac{1}{r_{p,0}^3} - \frac{1}{r_{e,0}^3}\right) \quad \text{(A-6a)}$$

$$\ddot{\delta}_g = \frac{\mu r_{e,0} \cos\sigma_0}{r_0} \left(\frac{1}{r_{p,0}^3} - \frac{1}{r_{e,0}^3}\right) \quad \text{(A-6b)}$$

$$\ddot{\alpha}_g = \frac{-\mu r_{e,0} \cos\delta_{s,0} \sin(\alpha_0 - \alpha_{s,0})}{r_0} \times \left(\frac{1}{r_{p,0}^3} - \frac{1}{r_{e,0}^3}\right) \quad \text{(A-6c)}$$

The nonzero partial derivatives in the matrix A_2 are given below:

$$\frac{\partial r}{\partial r_0} = 1 \quad \text{(A-7a)}$$

$$\frac{\partial r}{\partial \dot{r}_0} = t \quad \text{(A-7b)}$$

$$\frac{\partial \delta}{\partial \delta_0} = 1 \quad \text{(A-8a)}$$

$$\frac{\partial \delta}{\partial \dot{\delta}_0} = t \quad \text{(A-8b)}$$

$$\frac{\partial \alpha}{\partial \alpha_0} = 1 \tag{A-9a}$$

$$\frac{\partial \alpha}{\partial \dot{\alpha}_0} = t \tag{A-9b}$$

$$\frac{\partial \dot{r}}{\partial r_0} = \frac{\mu t(2 - 3\sin^2 \psi_0)}{{r_{p,0}}^3} + (\dot{\delta}_0^2 + \dot{\alpha}_0^2 \cos^2 \delta_0)t \tag{A-10a}$$

$$\frac{\partial \dot{r}}{\partial \delta_0} = -2tr_0\dot{\alpha}_0^2 \cos \delta_0 \sin \delta_0 + \mu t r_{e,0} \cos \sigma_0 \times \left(\frac{1}{{r_{p,0}}^3} - \frac{1}{{r_{e,0}}^3} - \frac{3r_0(r_0 - r_{e,0}\cos \chi_0)}{{r_{p,0}}^5}\right) \tag{A-10b}$$

$$\frac{\partial \dot{r}}{\partial \alpha_0} = \mu t r_{e,0} \cos \delta_0 \cos \delta_{s,0} \sin (\alpha_0 - \alpha_{s,0}) \times \left(\frac{1}{{r_{e,0}}^3} - \frac{1}{{r_{p,0}}^3} + \frac{3r_0(r_0 - r_{e,0}\cos \chi_0)}{{r_{p,0}}^5}\right) \tag{A-10c}$$

$$\frac{\partial \dot{r}}{\partial \dot{r}_0} = 1 \tag{A-10d}$$

$$\frac{\partial \dot{r}}{\partial \dot{\delta}_0} = 2r_0\dot{\delta}_0 t \tag{A-10e}$$

$$\frac{\partial \dot{r}}{\partial \dot{\alpha}_0} = 2r_0\dot{\alpha}_0 t \cos^2 \delta_0 \tag{A-10f}$$

$$\frac{\partial \dot{\delta}}{\partial r_0} = \frac{2t\dot{r}_0\dot{\delta}_0}{{r_0}^2} - \frac{t\ddot{\delta}_g}{r_0} + \frac{3\mu t r_{e,0}\cos \sigma_0}{{r_{p,0}}^5}\left(\frac{r_{e,0}}{r_0}\cos \chi_0 - 1\right) \tag{A-11a}$$

$$\frac{\partial \dot{\delta}}{\partial \delta_0} = -t\dot{\alpha}_0^2(\cos^2 \delta_0 - \sin^2 \delta_0) - \frac{t\ddot{\delta}_g \cos \chi_0}{\cos \sigma_0} + \frac{3\mu t {r_{e,0}}^2 \cos^2 \sigma_0}{{r_{p,0}}^5} \tag{A-11b}$$

$$\frac{\partial \dot{\delta}}{\partial \alpha_0} = \mu t r_{e,0} \cos \delta_{s,0} \sin (\alpha_0 - \alpha_{s,0}) \times \left[\frac{\sin \delta_0}{r_0}\left(\frac{1}{{r_{e,0}}^3} - \frac{1}{{r_{p,0}}^3}\right) - \frac{3{r_{e,0}}^2 \cos \delta_0 \cos \sigma_0}{{r_{p,0}}^5}\right] \tag{A-11c}$$

$$\frac{\partial \dot{\delta}}{\partial \dot{r}_0} = \frac{-2t\dot{\delta}_0}{r_0} \tag{A-11d}$$

$$\frac{\partial \dot{\delta}}{\partial \dot{\delta}_0} = 1 - \frac{2t\dot{r}_0}{r_0} \tag{A-11e}$$

$$\frac{\partial \dot{\delta}}{\partial \dot{\alpha}_0} = -2t\dot{\alpha}_0 \cos \delta_0 \sin \delta_0 \tag{A-11f}$$

$$\frac{\partial \dot{\alpha}}{\partial r_0} = \frac{2t\dot{r}_0\dot{\alpha}_0}{{r_0}^2} - \frac{t\ddot{\alpha}_g}{r_0 \cos \delta_0} + \frac{3\mu t r_{e,0}\cos \delta_{s,0}\sin (\alpha_0 - \alpha_{s,0})(r_0 - r_{e,0}\cos \chi_0)}{r_0 {r_{p,0}}^5 \cos \delta_0} \tag{A-12a}$$

$$\frac{\partial \dot{\alpha}}{\partial \delta_0} = \frac{t(2\dot{\delta}_0\dot{\alpha}_0 + \ddot{\alpha}_g \sin \delta_0)}{\cos^2 \delta_0} - \frac{3\mu t {r_{e,0}}^2 \cos \sigma_0 \cos \delta_{s,0}\sin (\alpha_0 - \alpha_{s,0})}{{r_{p,0}}^5 \cos \delta_0} \tag{A-12b}$$

$$\frac{\partial \dot{\alpha}}{\partial \alpha_0} = \frac{t\ddot{\alpha}_g}{\cos \delta_0(\tan \alpha_0 - \tan \alpha_{s,0})} + \frac{3\mu t {r_{e,0}}^2 \cos^2 \delta_{s,0}\sin^2 (\alpha_0 - \alpha_{s,0})}{{r_{p,0}}^5} \tag{A-12c}$$

$$\frac{\partial \dot{\alpha}}{\partial \dot{r}_0} = \frac{-2t\dot{\alpha}_0}{r_0} \tag{A-12d}$$

$$\frac{\partial \dot{\alpha}}{\partial \dot{\delta}_0} = 2t\dot{\alpha}_0 \tan \delta_0 \tag{A-12e}$$

$$\frac{\partial \dot{\alpha}}{\partial \dot{\alpha}_0} = 1 + \frac{2t(\dot{\delta}_0 \tan \delta_0 - \dot{r}_0)}{r_0} \tag{A-12f}$$

The matrix A_3 is used to make the transformation between a spherical coordinate system and a Cartesian plane-of-sky coordinate system. It is defined as follows:

$$A_3 = \begin{pmatrix} \frac{\partial r_{c,0}}{\partial r_0} & \frac{\partial r_{c,0}}{\partial \delta_0} & \frac{\partial r_{c,0}}{\partial \alpha_0} & \frac{\partial r_{c,0}}{\partial \dot{r}_0} & \frac{\partial r_{c,0}}{\partial \dot{\delta}_0} & \frac{\partial r_{c,0}}{\partial \dot{\alpha}_0} \\ \frac{\partial r_{\delta,0}}{\partial r_0} & \frac{\partial r_{\delta,0}}{\partial \delta_0} & \frac{\partial r_{\delta,0}}{\partial \alpha_0} & \frac{\partial r_{\delta,0}}{\partial \dot{r}_0} & \frac{\partial r_{\delta,0}}{\partial \dot{\delta}_0} & \frac{\partial r_{\delta,0}}{\partial \dot{\alpha}_0} \\ \frac{\partial r_{\alpha,0}}{\partial r_0} & \frac{\partial r_{\alpha,0}}{\partial \delta_0} & \frac{\partial r_{\alpha,0}}{\partial \alpha_0} & \frac{\partial r_{\alpha,0}}{\partial \dot{r}_0} & \frac{\partial r_{\alpha,0}}{\partial \dot{\delta}_0} & \frac{\partial r_{\alpha,0}}{\partial \dot{\alpha}_0} \\ \frac{\partial \dot{r}_{c,0}}{\partial r_0} & \frac{\partial \dot{r}_{c,0}}{\partial \delta_0} & \frac{\partial \dot{r}_{c,0}}{\partial \alpha_0} & \frac{\partial \dot{r}_{c,0}}{\partial \dot{r}_0} & \frac{\partial \dot{r}_{c,0}}{\partial \dot{\delta}_0} & \frac{\partial \dot{r}_{c,0}}{\partial \dot{\alpha}_0} \\ \frac{\partial \dot{r}_{\delta,0}}{\partial r_0} & \frac{\partial \dot{r}_{\delta,0}}{\partial \delta_0} & \frac{\partial \dot{r}_{\delta,0}}{\partial \alpha_0} & \frac{\partial \dot{r}_{\delta,0}}{\partial \dot{r}_0} & \frac{\partial \dot{r}_{\delta,0}}{\partial \dot{\delta}_0} & \frac{\partial \dot{r}_{\delta,0}}{\partial \dot{\alpha}_0} \\ \frac{\partial \dot{r}_{\alpha,0}}{\partial r_0} & \frac{\partial \dot{r}_{\alpha,0}}{\partial \delta_0} & \frac{\partial \dot{r}_{\alpha,0}}{\partial \alpha_0} & \frac{\partial \dot{r}_{\alpha,0}}{\partial \dot{r}_0} & \frac{\partial \dot{r}_{\alpha,0}}{\partial \dot{\delta}_0} & \frac{\partial \dot{r}_{\alpha,0}}{\partial \dot{\alpha}_0} \end{pmatrix} \tag{A-13}$$

The nonzero entries in the matrix A_3 are as follows:

$$\frac{\partial r_{c,0}}{\partial r_0} = 1 \tag{A-14}$$

$$\frac{\partial r_{\delta,0}}{\partial \delta_0} = r_0 \tag{A-15}$$

$$\frac{\partial r_{\alpha,0}}{\partial \alpha_0} = r_0 \cos \delta_0 \tag{A-16}$$

$$\frac{\partial \dot{r}_{c,0}}{\partial \delta_0} = -r_0 \dot{\delta}_0 \tag{A-17a}$$

$$\frac{\partial \dot{r}_{c,0}}{\partial \alpha_0} = -r_0 \dot{\alpha}_0 \cos^2 \delta_0 \tag{A-17b}$$

$$\frac{\partial \dot{r}_{c,0}}{\partial \dot{r}_0} = 1 \tag{A-17c}$$

$$\frac{\partial \dot{r}_{\delta,0}}{\partial r_0} = \dot{\delta}_0 \tag{A-18a}$$

$$\frac{\partial \dot{r}_{\delta,0}}{\partial \delta_0} = \dot{r}_0 \tag{A-18b}$$

$$\frac{\partial \dot{r}_{\delta,0}}{\partial \alpha_0} = r_0 \dot{\alpha}_0 \sin \delta_0 \cos \delta_0 \tag{A-18c}$$

$$\frac{\partial \dot{r}_{\delta,0}}{\partial \dot{\delta}_0} = r_0 \tag{A-18d}$$

$$\frac{\partial \dot{r}_{\alpha_0}}{\partial r_0} = \dot{\alpha}_0 \cos \delta_0 \tag{A-19a}$$

$$\frac{\partial \dot{r}_{\alpha,0}}{\partial \delta_0} = -r_0 \dot{\alpha}_0 \sin \delta_0 \tag{A-19b}$$

$$\frac{\partial \dot{r}_{\alpha,0}}{\partial \alpha_0} = \dot{r}_0 \cos \delta_0 - r_0 \dot{\delta}_0 \sin \delta_0 \tag{A-19c}$$

$$\frac{\partial \dot{r}_{\alpha,0}}{\partial \dot{\alpha}_0} = r_0 \cos \delta_0 \tag{A-19d}$$